J Mater Sci: Mater Electron (2013) 24:4060–4067
DOI 10.1007/s10854-013-1361-5

Formation of Cu_2SnS_3 thin film by the heat treatment of electrodeposited SnS–Cu layers

N. R. Mathews · J. Tamy Benítez · F. Paraguay-Delgado · M. Pal · L. Huerta

Received: 17 April 2013 / Accepted: 25 June 2013 / Published online: 13 July 2013

Abstract Thin films of copper tin sulfide (Cu_2SnS_3) were obtained by sulfurizing a stack of thin layers of Cu and SnS in nitrogen atmosphere. The film stack was obtained by the sequential electrodeposition of SnS and Cu. The Cu_2SnS_3 film was characterized for structural, morphological, composition, optical, spectroscopic, and electrical properties. The optimum condition for the formation of Cu_2SnS_3 was developed after testing different sulfurization temperatures. The films were polycrystalline with monoclinic structure which was confirmed by Raman and transmission electron microscopy analysis. The interplanar spacings estimated from the high resolution transmission electron microscopy images are 2.74, 2.19, and 2.06 Å. The average crystallite size is 13 nm, and the band gap of the film is in the range of 1 eV. The surface chemical composition determined by X-ray photoelectron spectroscopy showed the Cu:Sn:S ratio as 1.9:1:2.85 which is close to the stoichiometric Cu_2SnS_3. The films are *p*-type, photosensitive, and the conductivity measured in dark was in the range of $4 \times 10^{-3}\ \Omega^{-1}\ cm^{-1}$. The comprehensive characterization presented in this paper will update the knowledge on this material.

N. R. Mathews (✉) · J. Tamy Benítez · M. Pal
Instituto de Energías Renovables, Universidad Nacional Autónoma de México, 62580 Temixco, Morelos, Mexico
e-mail: nrm@cie.unam.mx

F. Paraguay-Delgado
Departamento de Materiales Nanoestructurados, Centro de Investigación en Materiales Avanzados (CIMAV), Chihuahua, Mexico

L. Huerta
Instituto de Investigaciones en Materiales, Universidad Nacional Autónoma de México, CP 04510 Mexico, DF, Mexico

1 Introduction

Semiconductors of the Cu–Sn–S system have gained considerable attention in recent years due to the abundance and the nontoxicity of the constituent elements. Different multicomponent phases such as Cu_2SnS_3 (CTS), $Cu_4Sn_7S_{16}$, Cu_3SnS_4, Cu_4SnS_4, $CuSn_{3.75}S_8$ etc. have been reported for this system. Among these ternary semiconducting sulfides, CTS is a promising material for solar cell applications due to its high absorption coefficient in the visible region and appropriate band gap for efficient solar-to-electric energy conversion. CTS have been reported to exist in different phases: cubic is a high temperature polymorph and other phases such as tetragonal and triclinic/monoclinic are formed at low temperatures [1, 2].

Different methods applied for the preparation of CTS has been reported. CTS in powder form was prepared by solvothermal [3], solid state reaction etc. [4], whereas thin films were deposited by spray pyrolysis [5, 6], sulfurization of sputter deposited [7], and electrodeposited metal precursors [1] followed by solid state reaction [8]. The estimated band gap energy is about 1.35 and 0.96 eV for tetragonal and cubic phases respectively, with a high absorption coefficient of 10^4 cm^{-1} in the visible region [7]. The first Schottky junction of CTS with indium was reported by Kuku et al. [9], with a power conversion efficiency of 0.11 % under 100 mW cm^{-2} incident radiation. Thin films of CTS incorporated into photovoltaic devices showed a power conversion efficiency of 0.54 %, short circuit current density of 17.1 mA cm^{-2}, and an open circuit voltage of 104 mV [10].

The aim of the present study is to develop stoichiometric CTS thin films by electrodeposition (ED) which is an economical method for the development of thin films for photovoltaic applications. We developed CTS films by the sequential electrodeposition of SnS and Cu films followed

by the annealing of this stack in nitrogen–sulfur atmosphere. Different techniques such as X-ray diffraction (XRD), scanning electron microscopy (SEM), energy dispersive X-ray spectroscopy (EDXS), high resolution transmission electron microscopy (HRTEM), X-ray photoelectron spectroscopy (XPS), photoconductivity and photoelectrochemical measurements, Raman spectroscopy, and optical transmittance spectroscopy were utilized to characterize the films.

Even though there are discussions on film growth and characterization for structural, optical, spectroscopic and morphological properties including demonstration of the photovoltaic activity mentioned above [1, 5, 7, 9–14], a comprehensive material study applying many characterization tools on the same batch of films is lacking in the literature. Such a detailed study using a single set of films is important since films prepared at different laboratories may vary in properties even if the film growth techniques are identical. In the present work we undertook an effort to characterize in detail the CTS films using different techniques mentioned above and the results presented in this paper will update the knowledge on this promising photovoltaic material.

2 Experimental

2.1 Deposition of thin films

The CTS thin films presented in this work were prepared by a two stage process. At first SnS and Cu thin films were sequentially electrodeposited on TCO (SnO_2:F) substrates, and then a sulfurization process was followed which resulted in the formation of CTS. The deposition of SnS was carried out by pulse electrodeposition as reported previously [15]. The Cu films were electrodeposited from an acidic bath containing 100 mM of $CuCl_2$ by applying a constant potential of −0.7 V versus saturated calomel electrode (SCE). The thickness of deposited SnS and Cu films was approximately 200 nm. The SnS–Cu stack was subjected to heat treatments in a vacuum furnace. First the chamber was evacuated to 10 mTorr and later heated to 100 °C while continuing pumping; this procedure was to eliminate the moisture. Subsequently, nitrogen was introduced to maintain the pressure at 10 Torr. The films were heat treated at different temperatures in N_2–S_2 atmosphere to optimize the formation of CTS. Purity of the sulfur powder utilized to generate the sulfur vapor was 99.99 %.

2.2 Characterization techniques

The XRD patterns of the thin films were recorded using a Rigaku D/MAX-2000 X-ray diffractometer with monochromatized Cu-Kα radiation (λ = 1.54056 Å) by scanning 2θ in the range 20°–70° at a grazing incidence angle of 0.5°. The Raman spectrum was recorded with a Labram Dilor micro Raman system by focusing the laser beam through a 50X microscope objective lense (spot diameter ~2 μ). The sample was excited with a He–Ne (332.6 nm) laser. The surface morphological analysis was carried out by employing a JEOL JSM7401F microscope. TEM micrographs were acquired with a Jeol JEM 2200FS with aberration corrected in the probe mode, and all the images were acquired in the scanning transmission electron microscopy (STEM) mode. The chemical analysis of the films was obtained using X-ray photoelectron spectroscopy (XPS). The XPS analysis was performed with a ultra-high vacuum (UHV) VG Microtech Multilab ESCA2000, with an Al Kα X-ray source (hν = 1486.6 eV). The surface of the film was etched for 15 min with 3.0 kV Ar+ at 0.06 μA mm^{-2}. The XPS spectrum was obtained at 55° to the normal in the constant pass energy mode E0 = 50 and 20 eV for survey and high resolution narrow scan. The peak positions were referenced to the background silver $3d_{5/2}$ at 368.20 eV, having a FWHM of 1.10 eV, and C 1*s* at 285.00 eV. The XPS spectra were fitted with the program SDP v 4.1 (SDP v 4.1 (32 bit) Copyright© 2004, XPS International, LLC, Compiled 17 January 2004). The surface elemental composition of Sn 3*d*, Cu 2*p*, S 2*p*, and O 1*s* core levels was determined with relative sensitivity factors (RSF) reported by Scofield and were corrected by the transmission function of the analyzer [16], and using the reference materials SnO, CuO, ZnO and ZnS.

The optical transmittance and reflectance spectrum was recorded using JascoV-670 spectrophotometer. The conductivity type of the CTS films was determined using photoelectrochemical (PEC) technique. For photo response measurements carbon electrodes were painted on the film surface and the measurement was carried out in a sandwich configuration (carbon electrode/CTS/conducting glass) using a Keithley 230 programmable voltage source and a Keithley 619 electrometer.

3 Results and discussion

3.1 Structural and morphological studies

The XRD patterns of the sequentially deposited SnS and Cu thin films are presented in the Fig. 1; (a) as deposited SnS–Cu films, (b) annealed at 300 °C and (c) annealed 350 °C. The reference patterns of the orthorhombic SnS (PDF 39-0354), Cu_2O (PDF 05-0667), CuS (PDF 06-0404) and monoclinic CTS (PDF 27-0198) are also included in the figure. Since the grazing incidence angle was 0.5° the XRD reflections corresponding to the SnO_2:F substrate are

too weak and are mostly absent in the XRD pattern. The X-ray diffraction patterns observed in Fig. 1a is mainly from SnS and Cu_2O. The films annealed at 300 °C shows the formation of binary phases SnS and CuS (Fig. 1b); however reflections which can be attributed to any ternary phases of Cu–Sn system was not observed. Hence it is clear that the reaction leading to the formation of ternary phase is not complete at these annealing conditions. In Fig. 1c the diffractions from (−2 −11), (−2 0 10), and (3 −2 10) planes at 28.4°, 47.25° and 56.06° are observed which corresponds to CTS, indicating that sulfurization at 350 °C for 30 min transforms the binary phases to ternary CTS compound. The peaks corresponding to SnS, Cu_2O and CuS phases have disappeared. The X-ray reflections from the binary phase Cu_8S_5 and CTS (patterns included in Fig. 1c) are very similar, hence the principal peak located at 28.4° (inset of Fig. 1c) was carefully examined. It can be clearly observed that the main XRD peak match better with the *d*-spacing of CTS than the Cu_8S_5.

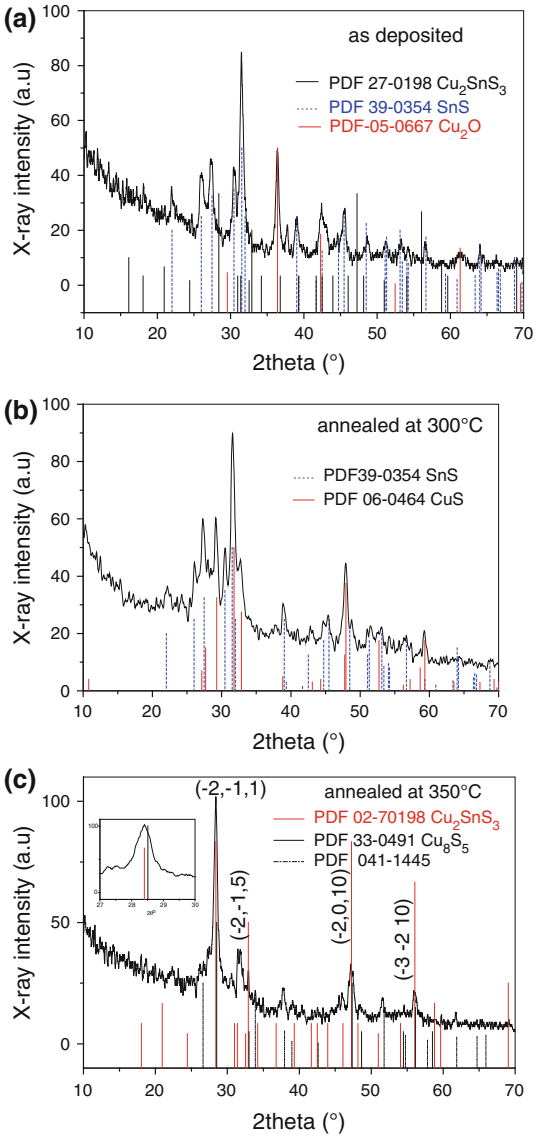

Fig. 1 X-ray diffraction patterns of: **a** as deposited SnS–Cu film along with the standard patterns of Cu_2SnS_3 (PDF 027-0198), SnS (PDF 39-0354), and Cu_2O (05-0667); **b** film annealed at 300 °C in N_2-S atmosphere with reference patterns SnS (PDF 39-0354) and CuS (PDF 06-0464); **c** film annealed at 350 °C in N_2-S with reference patterns of Cu_2SnS_3 (PDF 027-0198), Cu_8S_5 (PDF 33-0491) and cassiterite SnO_2 substrate (PDF 41-1445)

The average size of the CTS crystals was calculated using Scherer equation and full width at half maximum (FWHM) of (−2 −11) plane:

$$D = \frac{k\lambda}{\beta \cos\theta} \tag{1}$$

where D is the crystalline diameter, λ is the wavelength of the incident radiation, $k = 0.90$ is the shape factor, θ is the Bragg angle, and β is the FWHM in radians corresponding to Bragg angle θ. The calculated value of the average grain size was about 13 nm.

The preferential orientation of the crystallites along a crystal plane (hkl) can be indicated by the value of texture coefficient P_i (Eq. 2) [17]. The values of *P*i greater than unity indicate preferred orientation of the crystallites in that particular direction and less than unity indicates that the crystallites are randomly oriented.

$$P_i = \frac{N(I_i/I_{io})}{\sum_{i=1}^{N}(I_i/I_{io})} \tag{2}$$

where P_i is the texture coefficient of the plane *i*, *N* is the number of reflections taken for the analysis, I_i is the measured integral intensity of the reflection corresponding to the plane *i*, and I_{io} is the integral intensity of the powder diffraction pattern corresponding to the plane *i*. In order to estimate the preferential growth, four peaks of monoclinic CTS in the region $2\theta = 10°$–$70°$ was considered. The degree of the preferred orientation can be assessed by the standard deviation (σ); $\sigma = \sqrt{\frac{\sum_{i=1}^{N}(P_i - P_{io})}{N}}$ of all the P_i values. A value of zero for σ indicates that the sample is completely at random orientation. Table 1 shows the values of the texture coefficient and σ of the CTS thin film. Since the value σ is 0.4, we conclude that the film possesses no significant preference for a particular plane.

The surface morphology of the CTS films is studied by SEM and STEM imaging (Figs. 2 and 3). From SEM

Table 1 Texture coefficient and preferred orientation grade of the CTS film

Texture coefficient (P_i)					
	(−2 −1 1)	(−2 0 6)	(−2 0 10)	(−3 −2 10)	σ
CTS	1.41	0.33	0.35	0.22	0.4

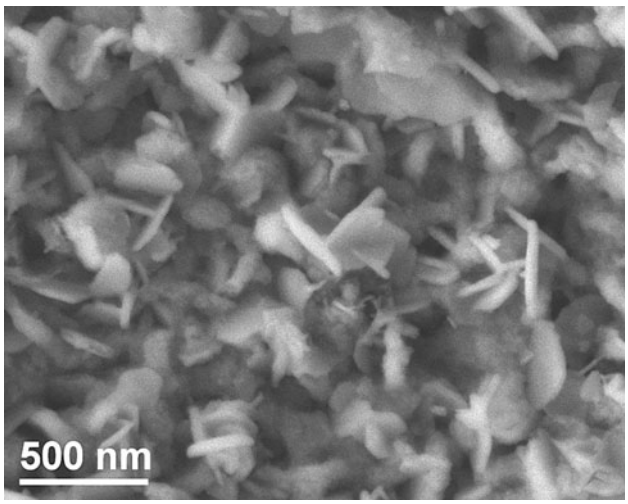

Fig. 2 Scanning electron microscope image of the Cu_2SnS_3 surface

image we can notice that the grains have platelet shape. The observed grains are agglomerations of various crystals.

The STEM micrographs are shown in Fig. 3. Figure 3a shows the bright field image, where the shape and the size of the agglomerated particles can be identified. These particles contained many crystals, and the morphology can be clearly seen in the image presented in Fig. 3b, which was acquired in the STEM mode using HAADF (high angle annular dark field) detector. Figure 3c shows the high resolution image of the grains and we can observe atomic columns and *d*-spaces of the crystallites. The fast Fourier transformation image is shown in the inset which shows periodicity of different *d*-spacing values. The values of *d*-spacing obtained from the FFT are shown in Fig. 3d which is a higher magnification image of Fig. 3c. The values of interplanar spacing 2.74, 2.19, and 2.06 Å are very close to

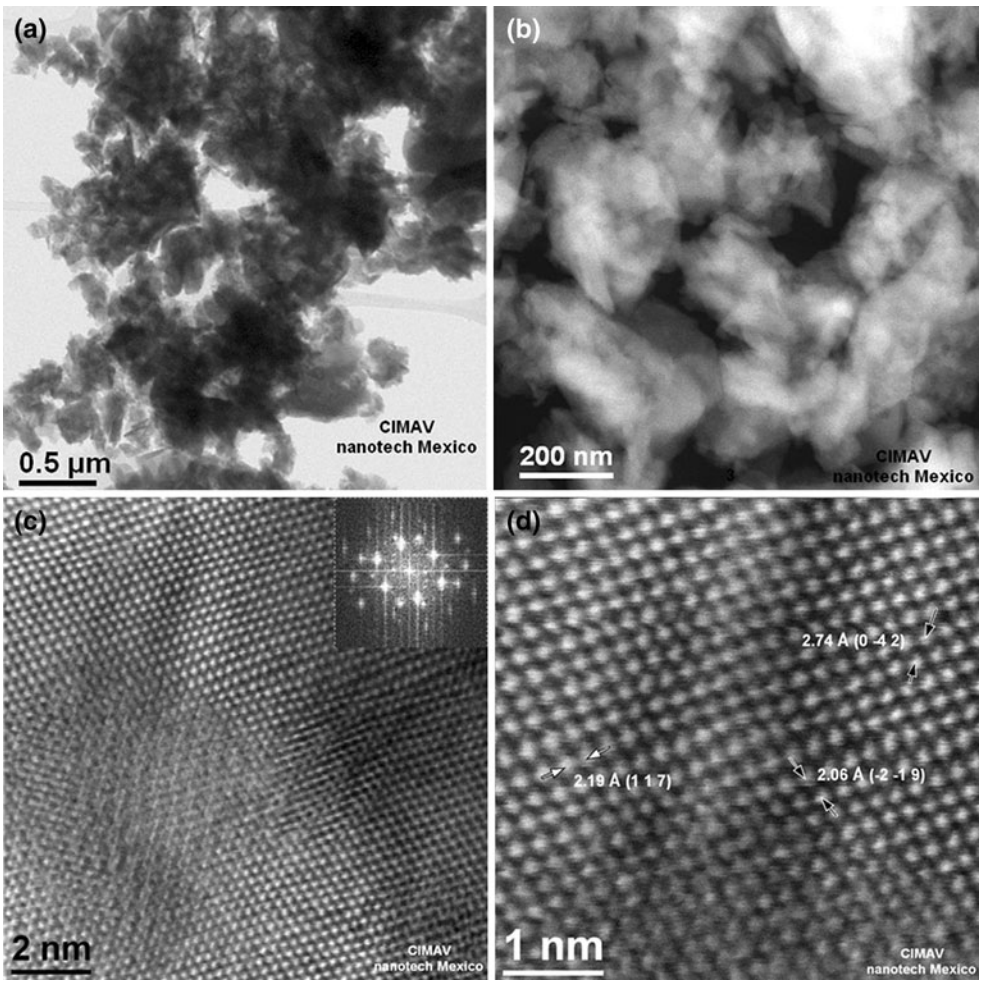

Fig. 3 Scanning transmission electron micrographs of Cu_2SnS_3: **a** bright field, **b** high angle annular dark field, **c** high resolution transmission electron microscopy with *inset* showing fast Fourier transformation image, and **d** d space measurements in the high resolution image

the PDF 27-0198 of the monoclinic CTS and correspond to (0 −4 2), (1 1 7), and (−2 −1 9) planes respectively.

The size of the crystallites was estimated from STEM micrographs; Fig. 4 shows the statistical distribution for all measurements. The particle size varied in a wide range; from particles of very small size of 2 nm to larger ones of 80 nm. However about 32 % of the particles demonstrated a size between 2 and 10 nm, which is in concordance with the data estimated from XRD.

3.2 Spectroscopic studies

Figure 5 shows the Raman spectrum of CTS thin films recorded in the range 50–400 cm^{-1}. The spectrum is

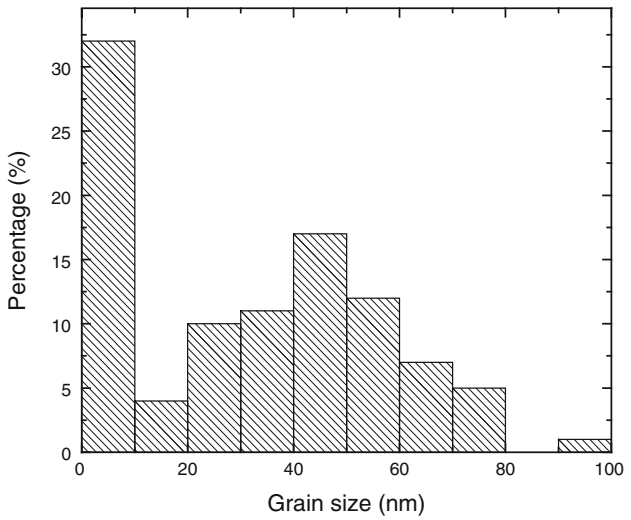

Fig. 4 Statistical distribution of grain size, the values were obtained from scanning transmission electron micrograph images

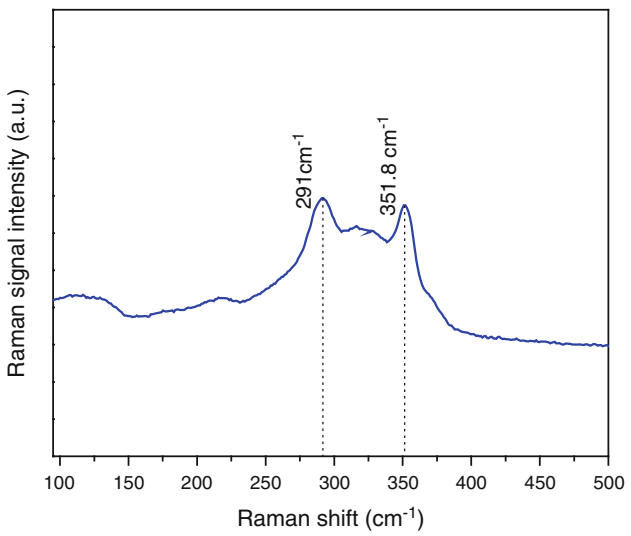

Fig. 5 Raman spectrum of the Cu_2SnS_3 thin film recorded in the spectral range of 100–500 cm^{-1}

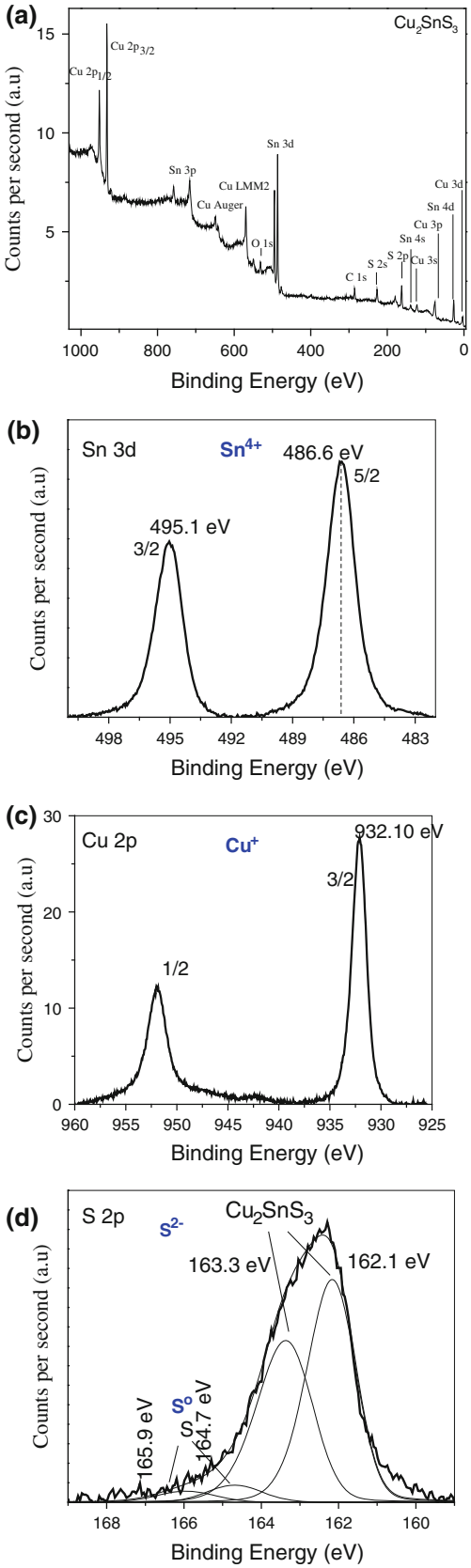

Fig. 6 X-ray photoelectron spectra of the Cu_2SnS_3 thin film: **a** survey scan, **b** Sn region, **c** Cu region, **d** S region

dominated by the presence of two Raman peaks at 291 and 353 cm^{-1}. The characteristic peak of $Cu_{2-x}S$ is reported at 475 cm^{-1} [18] and that of SnS are at 96, 163, 189, 220, and 288 cm^{-1} [19]. No bands are observed at the above mentioned positions, hence the presence of binary phases are excluded. Fernandes et al. [7] have reported the Raman band position for different Cu–Sn–S ternary phases. The Raman peaks reported for different CTS phases are at 336 and 351 cm^{-1} for tetragonal CTS; 303 and 355 cm^{-1} for cubic CTS; 290 and 352 cm^{-1} for the monoclinic CTS phase; and at 318, 348 and 295 cm^{-1} for Cu_3SnS_4. In the present study, Raman spectra showed peaks at 290 and 353 cm^{-1} which can be assigned to the Ao symmetry vibrational modes of monoclinic CTS as reported [1], which is in agreement with the XRD results discussed in Sect. 3.1.

The surface atomic composition and the presence of different possible components of Cu–Sn–S system in the films were analyzed using XPS. Figure 6a shows XPS survey spectrum of the CTS thin film, no signals for elemental copper, tin or sulfur were observed. The presence of Cu 2*p*, Sn 3*d*, O 1*s*, and S 2*p* peaks can be identified. The Sn 3*d* core level spectrum of CTS thin film is shown in Fig. 6b. The spectra show well-resolved doublet binding energies (BE) at 495.1 and 486.6 eV corresponding to Sn $3d_{5/2}$ and $3d_{3/2}$ respectively. These values are in agreement with the reported values of Sn^{4+} [12, 13] and no peaks of Sn^{2+} was observed. The Cu 2*p* core level spectrum is illustrated in the Fig. 6c, it can be observed that the binding energy values for Cu $2p_{3/2}$ (932.1 eV) and Cu $2p_{1/2}$ (952 eV) are similar to that reported for Cu^{+} [12, 20]. The satellite peak of Cu $2p_{3/2}$ which is characteristic of Cu^{2+} [21] is not present indicating the absence of any Cu^{2+}. The peaks at binding energies 162.1 and 163.3 eV correspond to S $2p_{3/2}$ and $2p_{1/2}$ respectively, characteristic of S^{2-} state of S atoms [14]. The present XPS analysis shows the valence states for CTS; $Cu_2^{2+}Sn^{4+}S_3^{2-}$. The surface chemical composition (at.%) determined by XPS is shown in Table 2. The Cu:Sn:S ratio 1.9:1:2.85 is close to the ideal value of CTS.

The optical transmittance (T) and reflectance (R) spectra of the CTS films recorded in the wavelength range 400–1500 nm are shown in the Fig. 7a. The optical absorption coefficient (α) at different wavelength was calculated from the following equation considering multiple reflections within the thin film.

$$\alpha = \frac{1}{d}\ln\left[\frac{(1-R)^2}{2T} + \left[\left(\frac{(1-R)^2}{2T}\right)^2 + R^2\right]^{\frac{1}{2}}\right] \quad (3)$$

Here T and R are the transmittance and reflectance values of the film at each wave length and d is the thickness of the film.

The band gap of a semiconductor can be calculated from absorption coefficient using the Tauc equation;

$$(\alpha h\nu)^n = A(h\nu - E_g) \quad (4)$$

where A is a constant, E_g is the band gap, and $h\nu$ is the photon energy. The value of n depends on the nature of electronic transitions during the absorption process; n = 2 or 2/3 in the case of direct allowed and forbidden transitions respectively. The values of $(\alpha h\nu)^2$ are plotted against

Table 2 The BE and chemical composition of CTS film determined by XPS

Cu_2SnS_3					
Cu (I) (2*p*)		Sn (IV) ($3d_{5/2}$)		S (2*p*)	
BE (eV)	Surf. conc. (at.%)	BE (eV)	Surf. conc. (at.%)	BE (eV)	Surf. conc. (at.%)
932.1	33.1	486.6	17.5	162.1	49.3

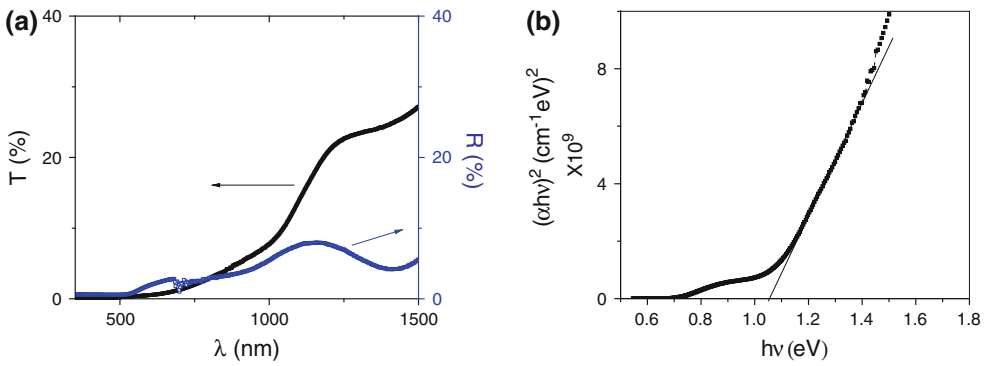

Fig. 7 **a** Optical transmittance and reflectance spectra of Cu_2SnS_3 thin film, **b** Plot of $(\alpha h\nu)^2$ versus hν for the estimation of band gap

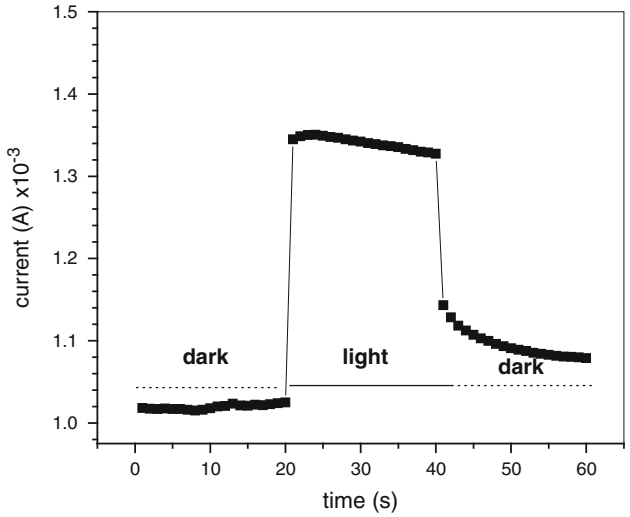

Fig. 8 Photocurrent response of Cu_2SnS_3 T thin films

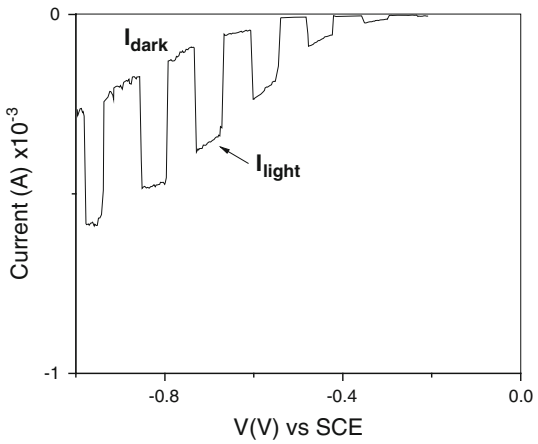

Fig. 9 Photoelectrochemical response under intermittent illumination, the increase in the cathodic current shows that the film is *p*-type

the values of photon energy (Fig. 7b) and a straight line region is observed over the photon energy range 1–1.7 eV. Thus, the optical gap is direct involving allowed transitions and the value was estimated as 1.05 eV. The reported values for the optical band gap of CTS is in the range of 0.9–1.3 eV depending on the crystal structure; 0.9 for cubic and 1.3 for tetragonal phase [7].

Figure 8 shows the photocurrent response of the CTS thin film. The electrical contact formation is explained in Sect. 2.2, the area of the electrical contact was 0.06 cm^2 (3 mm × 2 mm). The film was illuminated from TCO side. Prior to the measurements the sample was maintained in the dark under a constant applied potential of 0.1 V for about an hour to stabilize the current. Then the current was recorded at every second in the following sequence; 20 s in dark, 20 s in light and again 20 s in dark. The dark conductivity of the film was in the range of 4×10^{-3} Ω^{-1} cm^{-1}.

To investigate the conductivity type of the film, poto-electrochemical measurements (PEC) were carried out and the I–V curve is shown in Fig. 9. The cell used for this study was identical to that used for the electro deposition and the electrolyte was 0.1 M NaCl. The experiment was carried out under intermittent illumination produced using an optical chopper. A tungsten halogen lamp of intensity 100 mW cm^{-2} was used to illuminate the sample. The cathodic potential scan range was 0 to −1 V and we can observe an increase in the cathodic current (I_{light} in Fig. 9) indicating *p*-type conductivity for the film.

4 Conclusions

In this work, we achieved the formation of a ternary compound semiconductor, Cu_2SnS_3, by the eletrodeposition of SnS–Cu layers followed by an annealing process of the semiconductor–metal stack. The films were characterized for structural, morphological, composition, optical, spectroscopic, and electrical properties. XRD patterns showed that the films are monoclinic Cu_2SnS_3 without preferential orientation for a particular plane. The average crystallite size estimated from XRD data was 13 nm. The crystal structure and the particle size were confirmed by the TEM analysis. The XPS surface analysis showed the valence states for Cu_2SnS_3; $Cu_2^{2+}Sn^{4+}S_3^{2-}$. The surface chemical composition determined by XPS showed the Cu:Sn:S ratio as 1.9 :1: 2.85 which is close to the ideal value of Cu_2SnS_3. The optical band gap of the Cu_2SnS_3 film was 1.05 eV, which is comparable with the reported values. The films were photosensitive with *p*-type conductivity.

Acknowledgments The authors wish to thank Maria Luisa Ramón for the XRD measurements; O. Gomez Daza, G. Casarrubia Segura for general assistance in the chemical laboratory, José Campos for technical assistance in electrical studies. This work was partially supported by the projects PAPIIT IA100712, CONACyT-123122, and CONACyT-129169.

References

1. D.M. Berg, R. Djemour, L. Gutay, S. Siebentritt, P.J. Dale, X. Fontane, V. Izquierdo-Roca, A. Pérez-Rodriguez, Raman analysis of monoclinic Cu_2SnS_3 thin films. Appl. Phys. Lett. **100**, 192103 (2012)
2. X.A. Chen, H. Wada, A. Sato, M. Mieno, Synthesis, electrical Conductivity, and crystal structure of $Cu_4Sn_7S_{16}$ and structure refinement of Cu_2SnS_3. J. Solid State Chem. **139**, 144 (1998)
3. B. Li, Y. Xie, J. Huang, Y. Qian, Synthesis, characterization, and properties of nanocrystalline Cu_2SnS_3. J. Solid State Chem. **153**, 170 (2000)
4. M. Onoda, X. Chen, A. Sato, H. Wada, Crystal structure and twinning of monoclinic Cu_2SnS_3. Mater. Res. Bull. **35**, 1563 (2000)

5. M. Adelifard, M. Mehdi, B. Mohagheghi, H. Eshghi, Preparation and characterization of Cu_2SnS_3 ternary semiconductor nanostructures via the spray pyrolysis technique for photovoltaic applications. Phys. Scr. **85**, 035603 (2012)
6. M. Bouaziz, M. Amlouk, S. Belgacem, Structural and optical properties of Cu2SnS3 sprayed thin films. Thin Solid Films **517**, 2527 (2009)
7. P.A. Fernandes, P.M.P. Salom, A.F. da Cunha, Study of ternary Cu_2SnS_3 and Cu_3SnS_4 thin films prepared by sulfurizing stacked metal precursors. J. Phys. D Appl. Phys. **43**, 215403 (2010)
8. M. Bouaziz, J. Ouerfelli, S.K. Srivastava, J.C. Bernède, M. Amlouk, Growth of Cu_2SnS_3 thin films by solid reaction under sulphur atmosphere. Vacuum **85**, 783 (2011)
9. T. Kuku, O. Fakolujo, Photovoltaic characteristics of thin films of Cu_2SnS_3. Sol. Energy Mater. **16**, 199 (1987)
10. D.M. Berg, R. Djemour, L. Gütay, G. Zoppi, S. Siebentritt, P.J. Dale, Thin film solar cells based on the ternary compound Cu_2SnS_3. Thin Solid Films **520**, 6291 (2012)
11. Q. Lia, Y. Ding, X. Liu, Y. Qiana, Preparation of ternary I–IV–VI nanocrystallines via a mild solution route. Mater. Res. Bull. **36**, 2649 (2001)
12. X. Chen, X. Wang, C. An, J. Liu, Y. Qian, Preparation and characterization of ternary Cu–Sn–E (E = S, Se) semiconductor nanocrystallites via a solvothermal element reaction route. J. Cryst. Growth **256**, 368 (2003)
13. B. Li, Y. Xie, J. Huang, Y. Qian, J. Solid State Chem. **153**, 170 (2000)
14. M. Bouaziz, K. Boubaker, M. Amlouk, S. Belgacem, Effect of Cu/Sn concentration ratio on the phase equilibrium-related properties of Cu–Sn–S sprayed materials. J. Phase Equilib. Diff. **31**, 498 (2010)
15. N.R. Mathews, H.B.M. Anaya, M.A. Cortes Jácome, C. Angelez-Chavez, J.A. Toledo-Antonio, Tin sulfide thin films by pulse electrodeposition: structural, morphological, and optical properties. J. Electrochem. Soc. **157**, H337 (2010)
16. J.H. Scofield, Hartree–Slater subshell photoionization cross-sections at 1254 and 1487 eVJ. J. Electron. Spectros. Relat. Phenomena. **8**, 129 (1976)
17. C.S. Barrett, T.B. Massalski, *Crystallographic methods, principles and data*, 3rd edn. (McGraw Hill, NY, 1966), p. 205
18. P.A. Fernandes, P.M.P. Salome, A.F. da Cunha, Growth and Raman scattering characterization of Cu_2ZnSnS_4 thin films. Thin Solid Films **517**, 2519 (2009)
19. I.P. Parkin, L.S. Price, T.G. Hibbert, K.C. Molloy, The first single source deposition of tin sulfide coatings on glass: aerosol-assisted chemical vapour deposition using $[Sn(SCH_2CH_2S)_2]$. J. Mater. Chem. **11**, 1486 (2001)
20. C.D. Wagner, W.M. Riggs, L.E. Davis, J.F. Moulder, G.E. Muilenberg, *Handbook of XPS* (Perkin-Elmer Corporation, Eden Prairie, MN, 1979)
21. L.D. Partain, R.A. Schnerder, L.F. Donaghey, P.S. Meleod, Surface chemistry of CuxS and CuxS/CdS determined from X-ray photoelectron spectroscopy. J. Appl. Phys. **57**, 5056 (1985)